Check for updates

The Deubiquitinase OTU5 Regulates Root Responses to Phosphate Starvation[1][OPEN]

Der-Fen Suen,[a,2] Yi-Hsiu Tsai,[a] Ya-Tan Cheng,[a] Ramalingam Radjacommare,[b,c] Ram Nivas Ahirwar,[b,c] Hongyong Fu,[a,d,3] and Wolfgang Schmidt[a,d,e,3]

[a]Institute of Plant and Microbial Biology, Academia Sinica, 11529 Taipei, Taiwan
[b]Molecular and Biological Agricultural Sciences Program, Taiwan International Graduate Program, Academia Sinica, 11529 Taipei, Taiwan
[c]Graduate Institute of Biotechnology, National Chung-Hsing University, 402 Taichung, Taiwan
[d]Biotechnology Center, National Chung-Hsing University, 402 Taichung, Taiwan
[e]Genome and Systems Biology Degree Program, College of Life Science, National Taiwan University, 10617 Taipei, Taiwan

ORCID IDs: 0000-0002-4868-8284 (D.-F.S.); 0000-0002-2713-6034 (R.R.); 0000-0003-0567-3282 (R.N.A.); 0000-0002-7850-6832 (W.S.).

Phosphorus, taken up by plants as inorganic phosphate (Pi), is an essential but often growth-limiting mineral nutrient for plants. As part of an orchestrated response to improve its acquisition, insufficient Pi supply triggers alterations in root architecture and epidermal cell morphogenesis. Arabidopsis (*Arabidopsis thaliana*) mutants defective in the expression of the *OVARIAN TUMOR DOMAIN-CONTAINING DEUBIQUITINATING ENZYME5* (*OTU5*) exhibited a constitutive Pi deficiency root phenotype, comprising the formation of long and dense root hairs and attenuated primary root growth. Quantitative protein profiling of *otu5* and wild-type roots using the isobaric tag for relative and absolute quantification methodology revealed genotype- and Pi-dependent alterations in protein profiles. In *otu5* plants, Pi starvation caused a short-root-hair phenotype and decreased abundance of a suite of Pi-responsive root hair-related proteins. Mutant plants also showed the accumulation of proteins involved in chromatin remodeling and altered distribution of reactive oxygen species along the root, which may be causative for the alterations in root hair morphogenesis. The root hair phenotype of *otu5* was synergistic to that of *actin-related protein6* (*arp6*), harboring a mutation in the SWR1 chromatin-remodeling complex. Genetic analysis of *otu5/arp6* double mutants suggests independent but functionally related roles of the two proteins in chromatin organization. The root hair phenotype of *otu5* is not caused by a general up-regulation of the Pi starvation response, indicating that OTU5 acts downstream of or interacts with Pi signaling. It is concluded that OTU5 is involved in the interpretation of environmental information, probably by altering chromatin organization and maintaining redox homeostasis.

Phosphorus is an essential structural component of nucleic acids, ATP, and cell membranes and plays pivotal roles in signaling and catalytic reactions in metabolism. In plants, phosphorus is taken up as inorganic phosphate (Pi), which has limited phytoavailability in most ecosystems and agricultural settings due to complex interactions with soil constituents. Plants, in particular genera that do not engage in mycorrhizal symbiosis, have evolved sophisticated strategies to cope with low Pi availability involving metabolic, physiologic, and developmental responses, which aid in improving the acquisition, uptake, and distribution of Pi (Chiou and Lin, 2011).

Due to limited diffusion and mass flow of Pi in the soil solution, increasing the absorptive surface of the root is an efficient strategy to improve Pi acquisition and uptake. In Arabidopsis (*Arabidopsis thaliana*), Pi starvation induces coordinated alterations in root architecture that comprise the attenuation of primary root growth and an increase in lateral root formation, a response that has been referred to as topsoil foraging. The restricted longitudinal elongation of epidermal cells increases the number of root hairs per unit of root length in permissive positions (over anticlinal walls of cortical cells [H position]; Ma et al., 2001; Savage et al., 2013). In addition, Pi deficiency induces hair fate assignment in positions that are normally occupied by nonhair cells (above periclinal walls of underlying cortical cells [N position]; Ma et al., 2001; Müller and Schmidt, 2004). Root hairs formed in

[1] This work was supported by grants from Academia Sinica to H.F. and W.S. (AS-102-TP-B05) and the Ministry of Science and Technology to H.F. (MOST 105-2311-B-001-054).

[2] Current address: Agricultural Biotechnology Research Center, Academia Sinica, 11529 Taipei, Taiwan.

[3] Address correspondence to hongyong@gate.sinica.edu.tw or wosh@gate.sinica.edu.tw.

The author responsible for distribution of materials integral to the findings presented in this article in accordance with the policy described in the Instructions for Authors (www.plantphysiol.org) is: Wolfgang Schmidt (wosh@gate.sinica.edu.tw).

D.-F.S., H.F., and W.S. designed the research; D.-F.S., Y.-H.T., Y.-T.C., H.F., R.R., R.N.A., and W.S. performed the research; W.S. wrote the article.

[OPEN] Articles can be viewed without a subscription.
www.plantphysiol.org/cgi/doi/10.1104/pp.17.01525

 © 2018 American Society of Plant Biologists. All Rights Reserved.

response to Pi starvation are markedly longer than those formed under Pi-replete conditions, contributing to the increase in absorptive surface area of the root (Ma et al., 2001; Müller and Schmidt, 2004; Datta et al., 2015).

A relatively large subset of Pi-responsive genes has been associated with root hair formation, most of which play critical roles in root hair initiation and morphogenesis also under Pi-replete conditions (Lin et al., 2011; Salazar-Henao et al., 2016). In addition, forward genetic screens and genome-wide association mapping aimed at identifying genes that are particularly important for the root hair phenotype typical of Pi-deficient plants revealed novel players that are not regulated at the transcriptional level (Li et al., 2010; Chandrika et al., 2013; Stetter et al., 2015). For example, UBIQUITIN-SPECIFIC PROTEASE14 (UBP14/PER1) and the nucleus-localized plant homeodomain-containing protein ALFIN-LIKE6 (AL6/PER2) have been identified as regulators of root hair formation during Pi starvation (Li et al., 2010; Chandrika et al., 2013). Both *al6* and *ubp14* plants form very short root hairs under Pi-deficient conditions, but no deviations in root hair length from the wild type were apparent when grown in Pi-replete conditions. Mutants defective in *ACTIN-RELATED PROTEIN6* (*ARP6*), an essential component of the SWR1 chromatin-remodeling complex (Choi et al., 2007; Smith et al., 2010), show a constitutive Pi deficiency root hair phenotype. In *arp6* plants, compromised deposition of the histone variant H2A.Z resulted in the activation of several PSR genes, which is causally related to the root hair phenotype of the mutant (Smith et al., 2010).

Deubiquitinating enzymes (DUBs) are proteases that cleave ubiquitin from proteins. DUBs play multiple roles in cellular processes related to protein turnover and signaling. They are essential for the activation and recycling of ubiquitin, proofreading of ubiquitin-protein conjugates, maintenance of a free ubiquitin pool in cells, and fine-tuning the protein abundance by the removal of ubiquitin from modified proteins. In Arabidopsis, DUBs were shown to be involved in various cellular processes, including auxin signaling, development, and chromatin modification (Yang et al., 2007; Sridhar et al., 2007; Krichevsky et al., 2011).

Ovarian tumor domain (OTU)-containing DUBs belong to one out of five distinct classes of eukaryotic DUBs (Isono and Nagel, 2014), a family that is largely uncharacterized in Arabidopsis. So far, the only OTU-containing DUB in Arabidopsis with a well-defined function is OTUBAIN-LIKE DEUBIQUITINASE1, which can bind to chromatin and catalyze the deubiquitination of histone H2B in a gene repressor complex (Krichevsky et al., 2011). In an attempt to uncover novel roles of OTUs in plants, we initiated the characterization of the 12 OTU-containing DUBs in Arabidopsis (Radjacommare et al., 2014). Here, we report on the proteomic profile of a mutant defective in the expression of one gene from this family, *OTU5*. Mutants with compromised *OTU5* expression produce shorter primary roots and form longer and more frequent root hairs than wild-type plants, phenotypes that are typical of Pi-deficient plants. In addition, *otu5* plants form fewer lateral roots when compared with the wild type. Based on phenotypical characterization and protein profiling experiments, we conclude that the phenotype of *otu5* is caused by alterations in chromatin organization and the altered activity of a suite of genes involved in root hair morphogenesis and redox homeostasis.

RESULTS

OTU5 Is a Negative Regulator of Root Hair Morphogenesis Acting Independently of ARP6

The root phenotype of *otu5* mutants deviates from that of the wild type in several respects. First, *otu5* roots form significantly (36%) more root hairs per unit of root length than the wild type (Fig. 1). The *otu5* mutant used in this study is a T-DNA-inserted knockout mutant (Salk_032407) for which the full-length transcript and protein expression could not be detected. Mutant plants complemented with an N-terminal GST-tagged wild-type copy of the gene (*OTU5/otu5*) showed a phenotype similar to the wild type (Fig. 1). An analysis of the positions of root hairs in wild-type and *otu5* plants revealed that, in *otu5* roots, the formation of root hairs in the H position was increased by 67%. Also, markedly more hairs were formed in ectopic (N) positions than in the wild type (Table I). In *otu5* plants, the number of H positions was increased by additional cell divisions, resulting in an increase in the number of cortical cells (Table I). Transgenic lines overexpressing *OTU5* under the control of the 35S cauliflower mosaic virus promoter (OTU5 OE) showed a root hair number that did not differ from that of the wild type (Fig. 1).

The phenotype of *otu5* resembles that of the *arp6* mutant, harboring a defect in an SWR1 chromatin-remodeling complex subunit (Choi et al., 2007; Smith et al., 2010). Similar to *otu5,* homozygous *arp6* plants formed significantly more root hairs than the wild type; no differences in root hair density were observed between *otu5* and *arp6* plants (Fig. 1). Double mutants defective in the expression of both genes (*otu5/arp6*) showed a synergistic phenotype with regard to root hair density, suggesting that OTU5 and ARP6 act independently in the same process. In addition to root hair frequency, root hairs of *otu5* plants were longer than those of wild-type plants (Fig. 1). Homozygous *arp6* plants formed significantly longer root hairs than *otu5* seedlings ($P < 0.001$). Similar to what has been observed for root hair density, a synergistic phenotype was observed for *otu5/arp6* double mutants with respect to root hair length.

As expected from the increase in root hair number, primary root length was reduced significantly in *otu5* plants, indicative of restricted longitudinal elongation of the root epidermal cells or decreased cell

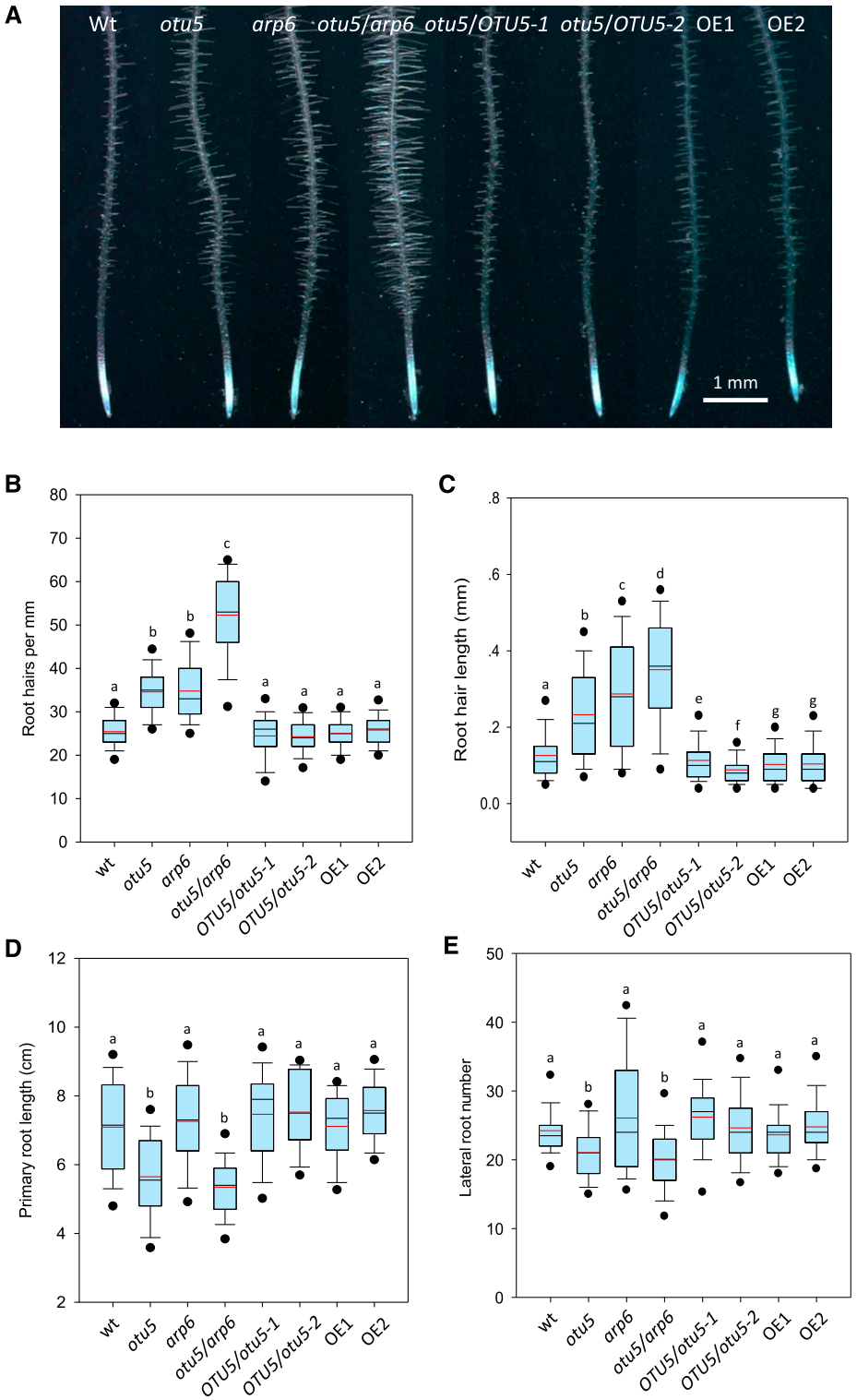

Figure 1. Root phenotypes under Pi-replete conditions. A, Micrographs of the root hair zone. B, Root hair density. C, Root hair length. D, Primary root length, E, Lateral root number. Black lines in the box plots indicate the median, and red lines indicate the mean. The 5th/95th percentiles of outliers are shown. A minimum of 100 root hairs from five roots were measured for each genotype and growth type. Different letters show significant differences at $P < 0.001$ inferred from one-way ANOVA on ranks analysis followed by Dunn's test. wt, Wild type.

proliferation (Fig. 1). No decrease in primary root growth was observed in *arp6*, suggesting that extra root hairs were due chiefly to the formation of hairs in ectopic positions. Double mutants defective in the expression of both *OTU5* and *ARP6* showed the *otu5* phenotype. No deviations from the wild type were observed in *otu5*/*OTU5* and OTU5 OE lines (Fig. 1). A similar picture emerged from the analysis of lateral root formation. While *otu5* and the *otu5/arp6* double mutant formed significantly fewer lateral roots, no difference from the wild type was observed for *arp6* and the OTU5 OE lines.

Table I. *Root cell type numbers in wild-type Col-0 and otu5 plants grown under control conditions (+Pi)*

Sample	Col-0	*otu5*
Epidermal cells	26.20 ± 0.09	27.18 ± 0.08
Cortical cells	8.24 ± 0.04	8.89 ± 0.03
Root hairs H position	0.84 ± 0.04	1.41 ± 0.06
Root hairs N position	0.004 ± 0.009	0.107 ± 0.016

Data were derived from more than 320 cross sections from eight roots (40 or more cross sections per root).

Roots of *otu5* Plants Show Altered Abundance of Chromatin- and Root Hair-Related Proteins

To identify proteins that are associated with the *otu5* phenotype, we surveyed the proteome of roots from wild-type and *otu5* mutant plants using the isobaric tag for relative and absolute quantification (iTRAQ) technology. In total, 10,328 proteins were identified and quantified, 490 of which accumulated differentially in *otu5* roots with 95% confidence intervals (1.302-fold for the up-regulated proteins and 0.755-fold for the down-regulated proteins; Fig. 2). Differentially expressed proteins are listed in Supplemental Data Set S1. A pronounced up-regulation (4.5-fold) was observed for the actin-like ATPase superfamily protein At2g42100. As a crucial component of the machinery that delivers material to the growing tip, the actin cytoskeleton plays an important role in cell expansion and in all stages of root hair development (Pei et al., 2012). Although At2g42100 localizes to the cytosol, it has predicted interactions with several proteins with nuclear localization, such as the chromatin-remodeling components ARP4, ARP5, and ARP6 (http://genemania.org). Furthermore, SNF2-RING-HELICASE-LIKE3 (FRG3), CHROMATIN REMODELLING8, and the histone H2A proteins HTA1 and HTA2, as well as TARGET OF RAPAMYCIN, a regulator of cell growth, showed increased abundance in *otu5* plants. Another protein with possible implications in the root hair phenotype of *otu5*, the xyloglucan-specific galacturonosyltransferase XUT1 (RHS8), showed highly increased abundance in *otu5* relative to the wild type (2.6-fold up).

A large subset of proteins showed decreased abundance in *otu5* plants. Notably, several proteins involved in chromatin remodeling, DNA methylation, histone modification, nucleosome assembly, and actin cytoskeleton organization were among the down-regulated proteins (Table II). Included in this group are the SET domain-containing proteins SU(VAR)3-9 HOMOLOG1 (SUVH1) and SUVH5 that have been associated with DNA/histone methylation, the chromatin remodeler SWC2, an SWR1 component homolog that interacts with H2A.Z (Choi et al., 2007), and HIGH MOBILITY GROUP B3, a protein involved in chromatin assembly/disassembly. These changes are indicative of altered chromatin organization in the *otu5* mutant. Also, another SNF2-RING-HELICASE-LIKE protein, FRG4, showed strongly decreased abundance in *otu5* mutants (Table II). FRG4 is an ortholog of FRG3, which was more abundant in *otu5* plants relative to the wild type. Together, the results suggest massive epigenetic alterations in the *otu5* mutant. Also, several proteins that are involved in cytoskeleton organization (At5g07740, ARPC5, and WAVE2) showed decreased abundance in roots of *otu5* plants. In addition to regulators of chromatin organization, proteins that have been associated with root hair morphogenesis, including the glycerophosphoryl diester phosphodiesterase-like protein GDPDL4/SHV3, an allele of the *shaven* mutant in which root hairs are ruptured during tip growth (Parker et al., 2000; Hayashi et al., 2008), the fasciclin-like arabinogalactan-protein FLA6, and the Pi starvation-induced glycerol-3-phosphate permease gene family protein GLYCEROL-

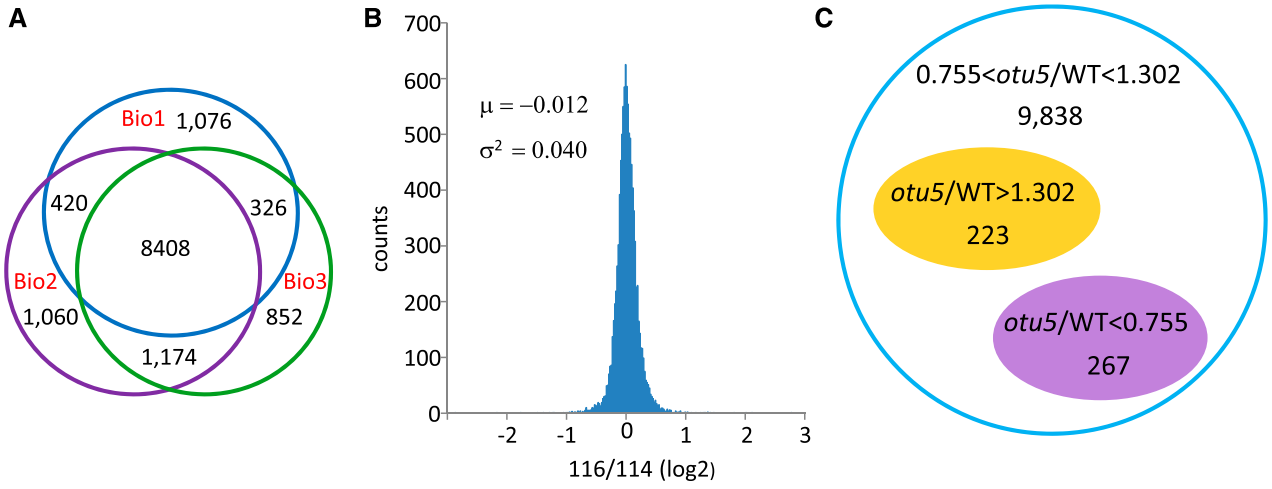

Figure 2. Protein identification in roots of *otu5* and the wild type (WT) under Pi-replete conditions. A, Venn diagram of the number of expressed proteins in three experimental runs (Bio1–Bio3). B, Distribution of protein abundance changes (iTRAQ counts) identified with false discovery rate (FDR) < 1%. C, Quantified differentially expressed proteins.

Table II. *Chromatin- and actin-related proteins that are differentially expressed between otu5 and wild-type plants ($P > 0.05$)*

Locus	Name	Function	Fold Change
otu5/wild type, Pi-replete conditions			
At3g16600	FRG3, SNF2-RING-HELICASE-LIKE3	DNA binding	2.61
At1g61140	FRG4, SNF2-RING-HELICASE-LIKE4	DNA binding	0.41
At2g18760	CHR8, CHROMATIN REMODELING8	DNA repair	1.56
At1g20696	HMGB3, HIGH MOBILITY GROUP B3	Chromatin assembly	0.73
At5g04940	SUVH1, SU(VAR)3-9 HOMOLOG1 (SET)	Histone methylation	0.71
At2g35160	SUVH5, (SGD9) SU(VAR)3-9 HOMOLOG5 (SET)	Histone methylation	0.74
At2g36740	SWC2	Chromatin remodeling	0.73
At4g01710	ARPC5, CROOKED	Actin cytoskeleton organization	0.75
At4g34940	ARMADILLO REPEAT ONLY1, ARO1	Actin cytoskeleton organization	1.33
At5g07740	Actin binding	Actin cytoskeleton organization	0.60
At1g29170	WAVE2	Actin cytoskeleton organization	0.63
At2g42100	Actin-like ATPase superfamily protein	Actin cytoskeleton	4.48
At5g54640	HTA1, HISTONE H2A1	Nucleosome assembly	1.46
otu5/wild type, Pi-deficient conditions			
At4g34290	SWIB/MDM2 domain superfamily protein	Chromatin remodeling	2.42
At5g23480	SWIB/MDM2 domain superfamily protein	Histone modification	2.40
At1g76710	SDG26, SET DOMAIN GROUP26	Histone methylation	2.11
At4g02020	SDG10, SET DOMAIN-CONTAINING PROTEIN10	DNA methylation	2.32
At2g42100	Actin-like ATPase superfamily protein		2.11
At1g70060	SNL4, SIN3-LIKE4	Histone deacetylation	3.25
At4g37280	MRG1, MORF RELATED GENE1	Chromatin remodeling	2.46
At3g12980	HAC5, HISTONE ACETYLTRANSFERASE OF THE CBP FAMILY5	Histone acetylation	2.01
At4g13570	HISTONE H2A 4, HTA4 (H2A.Z-like)	Nucleosome assembly	0.43

3-PHOSPHATE PERMEASE2, showed reduced abundance in *otu5* plants (Supplemental Data Set S1).

In *arp6* mutants, several Pi-responsive genes were up-regulated under Pi-replete conditions (Smith et al., 2010). To test whether this is also the case for *otu5*, we determined the expression of several markers for Pi starvation that are highly responsive to Pi starvation. Under control conditions, the abundance of NON-SPECIFIC PHOSPHOLIPASE C4 (NPC4; *otu5*:wild type ratio, 0.99), SPX DOMAIN GENE1 (SPX1; 1.13), and ULFOQUINOVOSYLDIACYLGLYCEROL2 (SQD2; 0.89) did not differ significantly between the genotypes. A comparison of the expression of these genes determined by qRT-PCR revealed a similar picture. As anticipated from previous studies, all tested genes were strongly up-regulated upon growth on low-Pi medium (Supplemental Fig. S1). In fact, the plasma membrane transporter *Pht1;2* was significantly down-regulated in Pi-replete *otu5* plants at the protein level, indicating Pi sufficiency. Furthermore, the production of anthocyanin, another indicator of the plant's Pi status, was not affected in Pi-replete *otu5* plants. Together, these results suggest that the overall Pi status is not affected by OTU5.

Pi Starvation Induces the Accumulation of Root Hair-Related Proteins in Wild-Type Roots

In wild-type plants, 637 proteins were responsive to growth on low-Pi medium. A subset of 382 proteins increased in abundance upon Pi deficiency, and 255 proteins were down-regulated (Fig. 3; Supplemental Data Set S1). Among the proteins with more than 2-fold increased abundance were mainly proteins involved in Pi uptake and recycling, such as the plasma membrane Pi transporters Pht1;1, Pht1;2, and Pht1;4, the regulator SPX1, proteins involved in membrane lipid remodeling (SQD1, SQD2, and PS2), and the purple acid phosphatase PAP17. Also, several proteins with validated roles in root hair formation are in this group, some of which showed strong Pi regulation at the protein level, such as the actin-binding formin homology family protein FH2 (3.4-fold), ROOT HAIR SPECIFIC13 (RHS13; 3-fold), the xyloglucan endotransglucosylase/hydrolases XTH26 (2.8-fold) and XTH14 (2.8-fold), MORPHOGENESIS OF ROOT HAIR6 (MRH6; 2.7-fold), SHV3-LIKE3 (2.6-fold), and the peroxidases RHS19 (2.2-fold), At1g05240 (2.2-fold), At4g26010 (2.7-fold), and At3g49960 (2.8-fold). All four peroxidases showed highly enriched transcript levels in root hairs over other root tissue (758-, 584-, 134-, and 81-fold, respectively; Lan et al., 2013). Notably, At1g05240 and At3g49960 have been identified previously as being critical for proper root hair elongation (Lan et al., 2013). Our quantitative proteome surveys also identified XUT1 (7.3-fold) as a novel player in the root hair morphogenesis of Pi-deficient plants. Mutants defective in the expression of *XUT1* produce a xyloglucan that lacks GalUA and form short root hairs, indicating that GalUA-containing xyloglucan is crucial for normal expansion of the hairs (Peña et al., 2012). *XUT1* has not been recognized as Pi responsive at the transcriptional level in previous transcriptomic surveys, suggesting that the abundance of XUT1 is chiefly or entirely posttranscriptionally regulated.

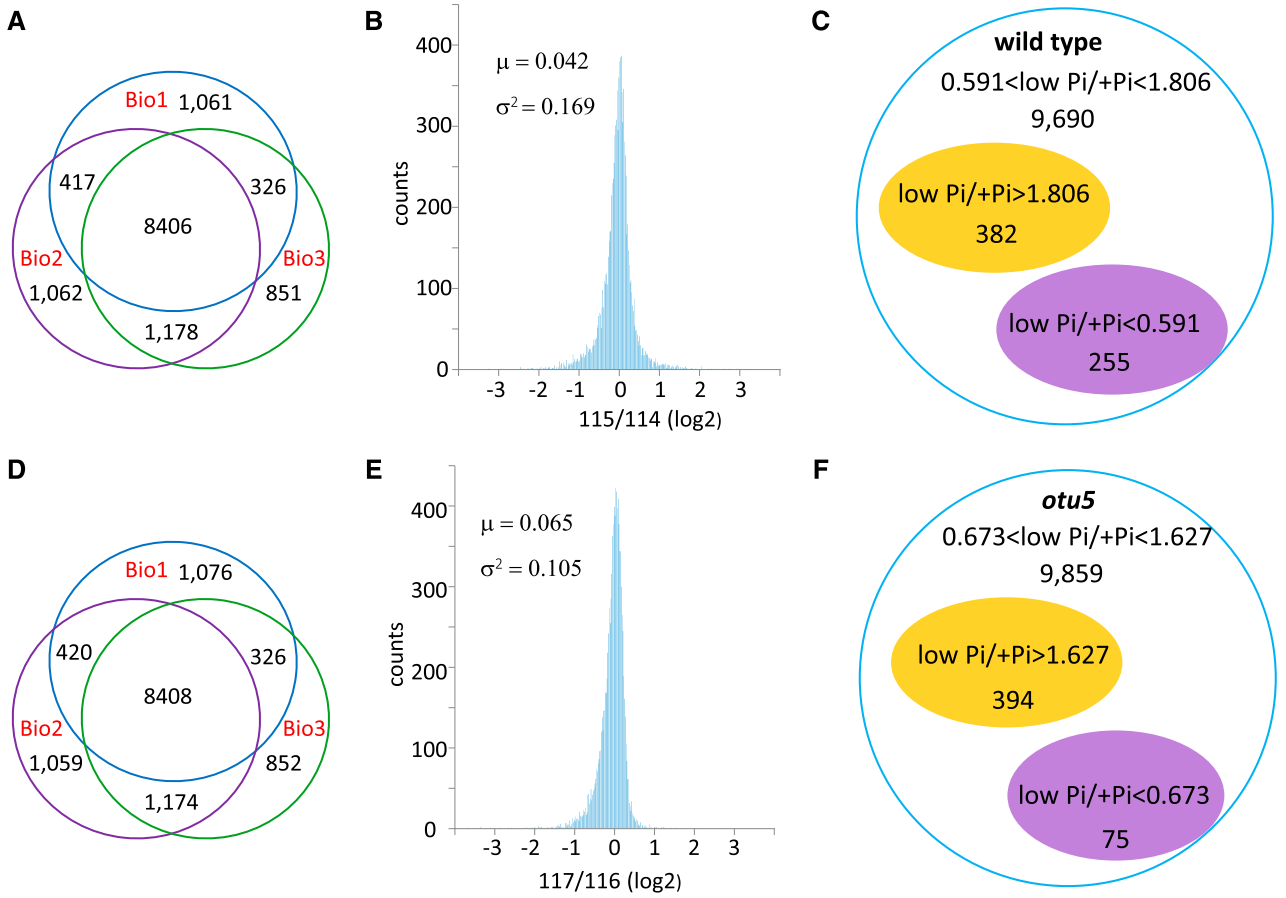

Figure 3. Protein identification in roots of *otu5* and the wild type under Pi-deficient conditions. A and D, Venn diagrams of the number of expressed proteins in three experimental runs (Bio1–Bio3) in the wild type (A) and *otu5* (D). B and E, Distribution of protein abundance changes (iTRAQ counts) identified with FDR < 1% in the wild type (B) and *otu5* (E). C and F, Quantified differentially expressed proteins in the wild type (C) and *otu5* plants (F).

Chromatin-Related Proteins Accumulate Differentially between *otu5* and Wild-Type Plants

Several chromatin-related proteins were responsive to Pi in the wild type, among them a subset that accumulated differentially between the *otu5* mutant and wild-type plants under control conditions (Table II). For example, FRG4 was strongly down-regulated by Pi starvation in wild-type roots (0.44-fold; Supplemental Data Set S1) but showed reduced abundance in the *otu5* mutant only under Pi-replete conditions (0.41-fold; Table II). Furthermore, the abundance of the histone deacetylase SIN3-LIKE4 (SNL4), the Polycomb group protein SET DOMAIN-CONTAINING PROTEIN10 (SDG10), and the chromatin remodeler MORF RELATED GENE1 (MRG1) was decreased in response to Pi starvation in the wild type, but the proteins were more abundant in the mutant relative to wild-type plants under these conditions. As a further example, the H2A.Z-like histone HTA4 (Yi et al., 2006) showed strongly reduced abundance in *otu5* plants under conditions of Pi deficiency when compared with the wild type but showed increased abundance in the wild type in response to Pi starvation. It thus appears that several chromatin-related proteins are regulated by Pi in a genotype-specific manner.

Integrated protein-protein interaction (PPI)/gene coexpression network analysis revealed that several of the proteins involved in chromatin remodeling that are deregulated in *otu5* are interconnected via PPIs and/or coexpressed with each other and with several genes involved in DNA-related processes such as histone modifications, DNA methylation, pre-mRNA splicing, chromatin assembly, and transcription (Fig. 4). It is obvious that several proteins/genes in this network are involved in the epigenetic regulation of reproductive development (i.e. MRG1, MRG2, VRN2, EMF2, ATO, and SDG26). It also appears that these genes are robustly expressed in roots at the protein level, which could be related to auxiliary roles of the encoded proteins in root development.

Since mutations in ARP6 are related to reduction of the histone variant H2A.Z in the chromatin of PSR genes, the synergistic phenotype of the two mutants

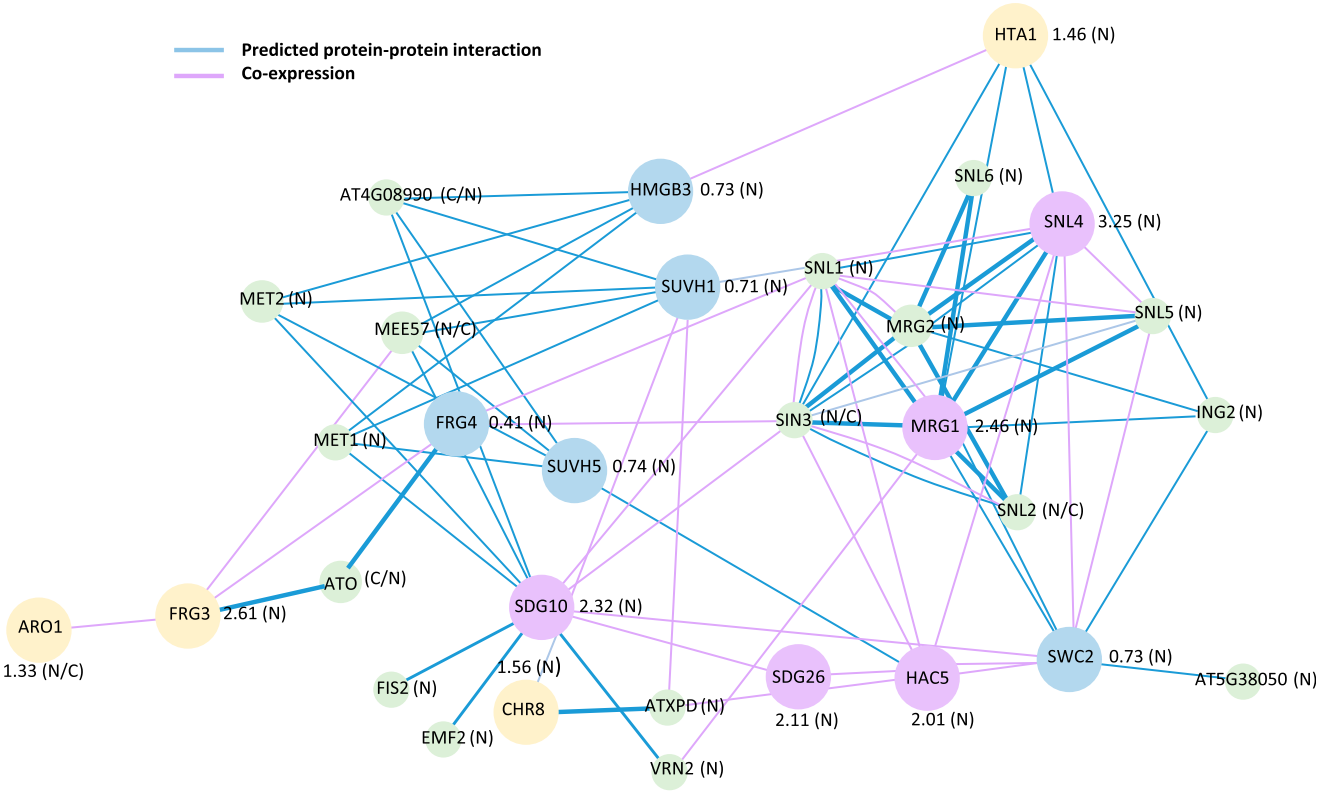

Figure 4. Integrated PPI and coexpression network of chromatin-related proteins. Proteins with functions in chromatin remodeling that accumulated differentially between *otu5* and wild-type plants were taken as bait to construct a network of interacting proteins and genes that are coexpressed with these proteins. The weight of the edges indicates the strength of the interactions. Yellow nodes indicate proteins with increased abundance, blue nodes denote proteins with decreased abundance, and purple nodes represent proteins that accumulate differentially under conditions of Pi deficiency. The smaller green nodes indicate genes that are coexpressed with these proteins. Letters in parentheses indicate the predominant location of the gene product: N, nucleus; C, cytoplasm. The network was constructed with GeneMANIA (http://genemania.org).

under investigation gives rise to the speculation that the phenotype of *otu5* is related to altered histone H2A.Z occupancy. To investigate this possibility, we determined the abundance of H2A.Z in two representative genes encoding differentially expressed proteins functioning either in root hair morphogenesis (XTH26) or chromatin remodeling (FRG4) by chromatin immunoprecipitation (ChIP)-qPCR. Both genes showed a significant reduction of H2A.Z in their chromatin upon Pi starvation in roots of the wild type (67% and 71% for XTH26 and FRG4, respectively; Supplemental Fig. S2), a phenomenon that has been observed previously for several PSR genes (Smith et al., 2010; Kuo et al., 2014). In both genes and both mutants under investigation, H2A.Z occupancy was reduced substantially, an effect that was slightly more pronounced in *arp6*. Pi starvation did not further reduce the abundance of H2A.Z.

Nonfunctional OTU5 Alters the Root Responses to Low Pi

As anticipated from previous studies (Ma et al., 2001; Müller and Schmidt, 2004), growing wild-type plants on low-Pi medium significantly increased the number of root hairs (Fig. 5). In *otu5* plants, the constitutively higher number of root hairs was further increased upon Pi starvation by 68% (Figs. 1 and 5). The increase in root hair density was caused by the formation of extra hairs in both H (by decreasing the longitudinal length of root epidermal cells) and N (by additional root hair cell fate assignment) positions (Table III). Both *otu5*/*OTU5* and OTU5 OE lines showed an increase in root hair number that was similar to that of the wild type (Fig. 5). The root hair density of *arp6* plants was increased by 81% upon Pi starvation (Figs. 1 and 5) and was significantly higher than that of *otu5* ($P < 0.001$). Similar to what has been observed under Pi-replete conditions, *otu5/arp6* double mutants showed a synergistic phenotype with respect to the root hair density (Fig. 5). In wild-type plants, root hair length was increased from 0.13 to 0.38 mm on average (Figs. 1 and 5). No Pi deficiency-induced increase in hair length was observed in *otu5* plants. For *arp6* and the *otu5/arp6* double mutant, a decrease rather than an increase in root hair length upon Pi starvation was observed (−29% and −65%, respectively). Also here, the two mutations acted synergistically on the elongation of the hairs (Fig. 5).

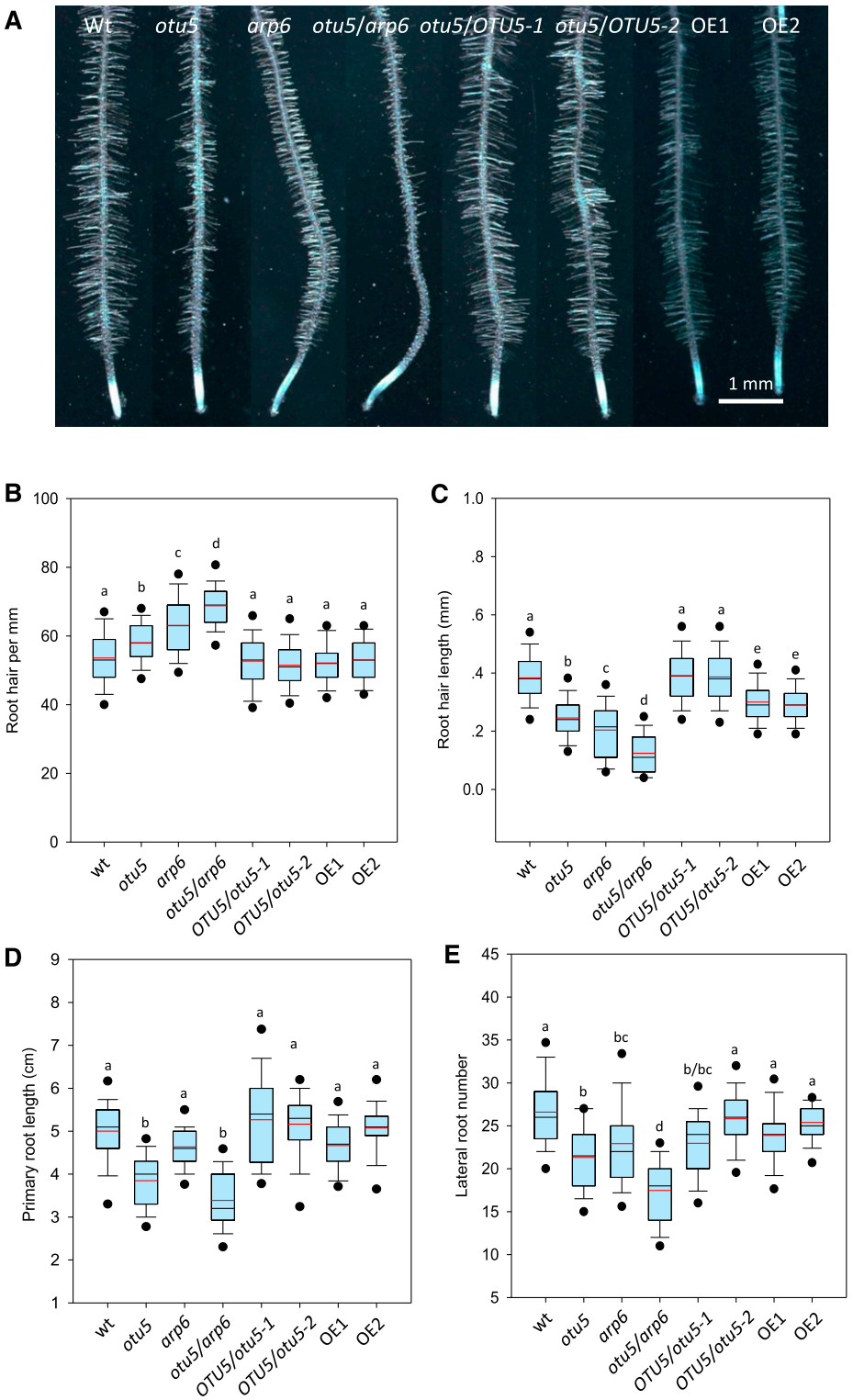

Figure 5. Root phenotypes under Pi-deficient conditions. A, Micrographs of the root hair zone. B, Root hair density. C, Root hair length. D, Primary root length. E, Lateral root number. Black lines in the box plots indicate the median, and red lines indicate the mean. The 5th/95th percentiles of outliers are shown. A minimum of 100 root hairs from five roots were measured for each genotype and growth type. Different letters show significant differences at $P < 0.001$ inferred from one-way ANOVA on ranks analysis followed by Dunn's test. wt, Wild type.

Growing plants on low-Pi medium attenuated the growth of primary roots. In *otu5* plants, primary root growth was more severely restricted than in the wild type. A significant decrease in primary root length also was observed for *arp6* plants, although to a lesser extent when compared with *otu5*; the *otu5/arp6* double mutant showed a synergistic phenotype (Fig. 5). A similar but more pronounced pattern was observed for lateral root formation. While wild-type plants showed an increase in lateral root number that is

Table III. *Root cell type numbers in wild-type and otu5 plants grown on low-Pi medium*

Sample	Col-0	*otu5*
Epidermal cells	27.89 ± 0.06	28.24 ± 0.08
Cortical cells	8.26 ± 0.02	8.86 ± 0.05
Root hairs H position	1.69 ± 0.06	1.96 ± 0.06
Root hairs N position	0.197 ± 0.021	0.261 ± 0.023

Data were derived from more than 320 cross sections from eight roots (40 or more cross sections per root).

typically observed in Pi-deficient plants, such an increase was not observed for *otu5* and *arp6* plants. Double mutants showed a pronounced decrease in lateral root formation. Similar to what has been observed for primary root length, no general trend was observed with respect to the number of lateral roots in OTU5 OE lines.

Chromatin-Related Proteins Are Deregulated in Pi-Deficient *otu5* Plants

While the number of proteins that showed increased abundance in response to Pi starvation in the *otu5* mutant was comparable to that of the wild type (394 versus 382), fewer proteins were down-regulated in *otu5* (75 versus 255; Fig. 3), suggesting that OTU5 acts as a repressor for a subset of Pi-responsive proteins. Among the up-regulated proteins, only 92 were commonly regulated in both genotypes. This group comprised several key players in the PSR (i.e. SQD1, Pht1;2, Pht1;4, SPX1, and PAP17) and several root hair-related proteins (i.e. FH2, RHS13, SLV3, XUT1, PRPL1, and XTH14; Supplemental Data Set S1).

PPI/coexpression analysis of the proteins that were solely Pi responsive in the mutant revealed a cluster that comprised several proteins/genes related to chromatin remodeling (Fig. 6). The histone H2A proteins HTA9, one of the H2A.Z-coding genes in Arabidopsis (Coleman-Derr and Zilberman, 2012), HTA7, and HTA12, as well as the histone H2B proteins HTB4 and HTB9, belong to this subset (Fig. 6). Further components of this cluster are the trithorax group protein ASH1-RELATED PROTEIN1 (SDG26) and the SWR1 component SWC2, which interacts with H2A.Z (Choi et al., 2007). Numerous interactions among histone family proteins suggest Pi deficiency-induced changes in histone composition in *otu5* plants.

Under Pi-deficient conditions, a subset of 304 proteins showed reduced abundance in the *otu5* mutant relative to the wild type. Several proteins with key functions in cellular Pi homeostasis that are highly Pi responsive in the wild type (i.e. SPX1, SQD2, Pht1;2, and Pht1;4) were less abundant in Pi-deficient *otu5* mutants. This finding is opposite to what has been observed with the *arp6* mutant, which showed increased expression of Pi-responsive genes under Pi-replete conditions. A large set of proteins, including the

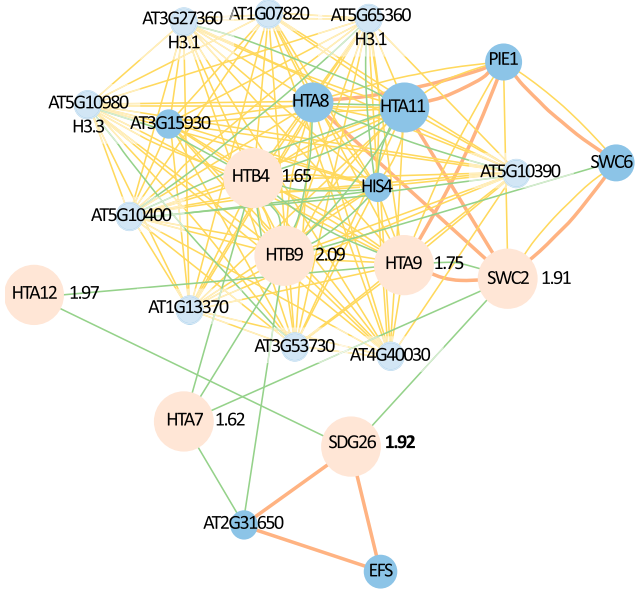

Figure 6. Integrated PPI and coexpression network of proteins that were Pi responsive in *otu5* but not in wild-type plants. Proteins that accumulated differentially between Pi-deficient and Pi-replete *otu5* plants were taken as bait to construct a network of interacting proteins and genes that are coexpressed with these proteins (yellow nodes). Blue nodes indicate genes that are coexpressed with these proteins. The weight of the edges indicates the strength of the interactions. Numbers indicate induction level (n-fold) by Pi starvation. The network was constructed with GeneMANIA (http://genemania.org).

chromatin-related proteins SNL4 (DMR), SDG10, and SDG26 and the SWIB/MDM2 domain proteins At4g34290 and At5g23480, was up-regulated under Pi-deficient conditions in *otu5* relative to wild-type plants. SNL4, SDG10, and At4g34290 were down-regulated upon Pi starvation in the wild type, supporting the genotype-specific regulation of chromatin and root hair-related proteins by the Pi supply.

A Cluster of Root Hair-Related Proteins Fails to Accumulate in *otu5* Roots in Response to Pi Starvation

Several root hair-related proteins, most of which were strongly up-regulated in the wild type under Pi deficiency, showed decreased abundance in Pi-deficient *otu5* plants relative to the wild type and, thus, may contribute to the *otu5* mutant phenotype under Pi-deficient conditions. This subset included the peroxidases At4g26010, At1g05240, RHS19, At3g49960, and At5g17820, the formins FH2 and FH8, RSH15, XTH14, XTH26, SLV3, FLA6, UCC3, and MRH6. For two other proteins, the plasma membrane intrinsic protein subfamily protein PIP2;4 and the peroxidase At3g49960, root hair phenotypes were reported previously for the corresponding mutants (Lin et al., 2011; Lan et al., 2013). Decreased protein abundance was observed in *otu5* mutants either under both growth conditions (PIP2;4) or only when grown on

low-Pi medium (At3g49960). Several proteins with decreased abundance in Pi-deficient *otu5* plants are expressed preferentially in root hairs (Lan et al., 2013), including the unknown protein At2g30930, the peroxidases At5g17820 and At1g05240, as well as FH2 and the membrane-anchored endo-1,4-β-D-glucanase KOR2, which showed lower abundance in the mutant only under Pi-deficient conditions. A subset of proteins from this group showed predicted or validated PPIs, suggesting that these proteins cooperatively induce the root hair phenotype typical of Pi-deficient plants (Fig. 7).

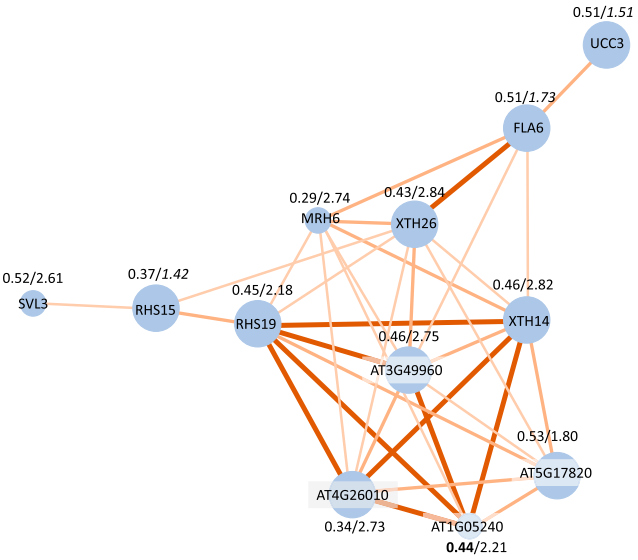

Figure 7. PPI network of root hair-related proteins with decreased abundance in *otu5* plants. The first number indicates the *otu5* low-Pi/wild-type low-Pi ratio of protein abundance, and the second number denotes the induction by Pi starvation in wild-type roots. Numbers in italics indicate nonsignificant changes. The weight of the edges indicates the strength of the interactions. The network was constructed with STRING (http://string-db.org).

OTU5 Maintains Reactive Oxygen Species Distribution in Roots

The distribution of reactive oxygen species (ROS) strongly affects the pattern and length of root hairs (Sundaravelpandian et al., 2013). Several proteins that may alter the redox homeostasis of root epidermal cells were differentially expressed between *otu5* and wild-type plants. To investigate a putative contribution of altered ROS distribution to the root hair phenotype of *otu5* plants, we analyzed the level and distribution of hydrogen peroxide (H_2O_2) and superoxide anions. H_2O_2 was detected by 3′-(*p*-hydroxyphenyl) fluorescein (HPF), which reacts with H_2O_2 by forming strongly fluorescent fluorescein (Setsukinai et al., 2003; Dunand et al., 2007). In the wild type, fluorescence was reduced when plants were grown on low-Pi medium in both the meristematic region and the elongation zone (Fig. 8). Fluorescence both in the root tip and in the elongation zone was significantly lower in roots of *otu5*, an effect that was most pronounced under conditions of Pi starvation, where H_2O_2 levels were reduced to approximately one-third of that in the wild type (Fig. 8C). Superoxide staining by nitroblue tetrazolium chloride (NBT) revealed perturbed distribution in *otu5* mutants, with lower formazan production in the meristematic region, while no differences to the wild type were observed in the differentiation zone (Fig. 8, D–F). Under low-Pi conditions, no decrease in superoxide accumulation was observed in the meristem of *otu5* plants (Fig. 8, D and F). The dramatically altered distribution of both ROS species in the presence of sufficient Pi might be causative for the long-root-hair phenotype observed for *otu5* under these conditions. Together, these results demonstrate that a mutation in *OTU5* causes massive and context-dependent perturbation of ROS homeostasis.

DISCUSSION

OTU5 Is Critical for the Interpretation of Environmental Information

Previous studies suggest that chromatin organization is important for root hair size and patterning in response to environmental signals. In addition, chromatin organization appears to be critical for a subset of the PSR responses. Mutants defective in the expression of the class I histone deacetylases *HDA6*, *HDA9*, and *HDA19* showed a less pronounced increase in root hair density upon growth on Pi-deplete medium (Chen and Schmidt, 2015). Similar to what has been observed for *arp6*, several Pi-responsive genes were deregulated in *hda19* knockdown lines (Chen and Schmidt, 2015). Chromatin-level regulation of Pi-induced root hair formation can be further inferred from the phenotype of the *per2/al6* mutant, defective in the expression of the plant homeodomain-containing protein AL6. AL6 binds to dimethylated or trimethylated Lys-4 on histone H3 (Lee et al., 2009) and may act in the processing of transcripts related to several aspects of the Pi starvation response (Chandrika et al., 2013).

Based on the observed alterations in protein profiles, it appears reasonable to speculate that perturbed control of the expression of chromatin-related proteins may be causative for the root hair phenotype of the *otu5* mutant. Several histone-related genes are part of a PPI/coexpression network obtained from bait proteins that are Pi responsive in *otu5* but not in the wild type. While chromatin-related proteins were mostly downregulated in *otu5* under Pi-replete conditions, several proteins from this group strongly accumulated when plants were grown on low-Pi medium (Table II). Thus, it can be inferred that OTU5 is required for the interpretation of external signals, which tunes the abundance of proteins that are relevant for the proper response to Pi starvation and root hair elongation, possibly by altering nucleosome positioning or by promoting posttranslational modifications of histones.

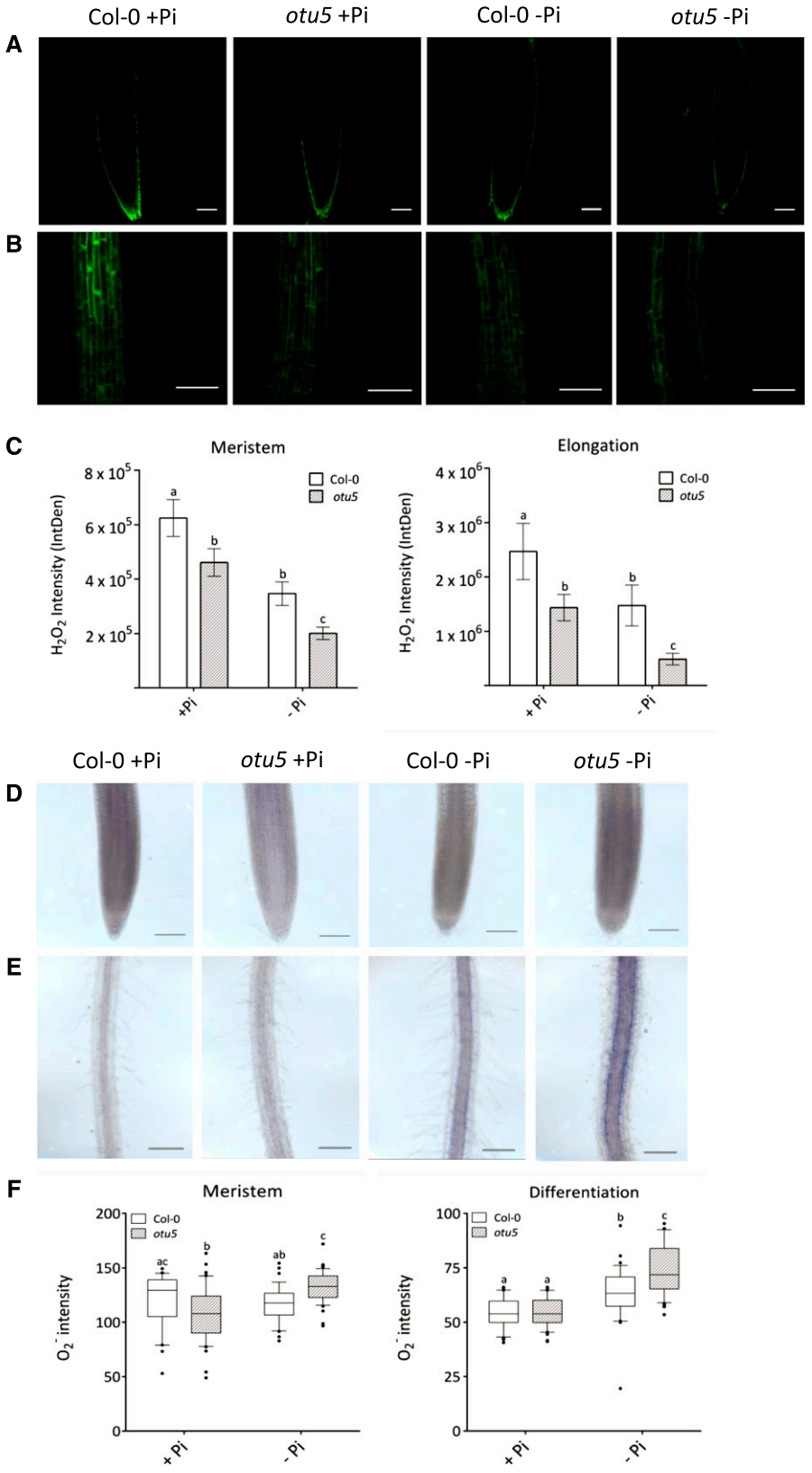

Figure 8. Distribution of ROS along the roots. A and B, Roots stained with HPF for H_2O_2 in the meristem (A) and elongation zone (B). Plants were stained for 2 min in 0.1 M phosphate buffer (pH 6.1) containing 5 μM HPF. C, Quantification of HPF fluorescence intensity. D and E, Roots of 14-d-old Arabidopsis plants stained with NBT for superoxide in the meristem (D) and differentiation zone (E). Roots were stained for 25 min in 20 mM phosphate buffer (pH 6.1) containing 2 mM NBT and subsequently destained for 40 min. F, Quantification of NBT staining intensity. Error bars represent SE; $n = 20$. Different letters indicate significant differences ($P > 0.05$) between samples as determined by two-way ANOVA and Tukey's (NBT) or Fisher's LSD (HPF) test. Bars = 100 μm; NBT differentiation zone = 200 μm.

Notably, homozygous *otu5* plants differentially accumulated several chromatin-related proteins that are related to flowering control, such as SWC2 (Choi et al., 2007), SDG10 (Wang et al., 2016), MRG1 (Xu et al., 2014), and SDG26, a methyltransferase that is required for trimethylation of Lys-4 and Lys-36 of histone 3 at the AGAMOUS-LIKE20 locus (Berr et al., 2015). Although pleiotropic defects in both vegetative and reproductive development have been reported for several mutants with flowering phenotypes (Pouteau et al., 2004), detailed phenotypic characterization of flowering-related mutants such as *arp4*, *swc6*, and *pie1* was restricted to aerial plant parts (Kandasamy et al., 2005; Lázaro et al., 2008; March-Díaz et al., 2008). Thus, a potential involvement of these genes in environmentally induced adaptations in root hair formation via epigenetic alterations may have remained unnoticed.

Perturbed Redox Homeostasis May Contribute to the Root Hair Phenotype of *otu5*

A finding that is puzzling at first sight is that the two mutations synergistically increased root hair density independently of the Pi supply, while root hair length followed opposite trends in Pi-replete and Pi-deficient plants. This observation, however, is in line with the oppositional regulation of a suite of root hair-related proteins in Pi-deficient wild-type and *otu5* plants. This subset, which can be considered as a functional module mediating Pi deficiency-induced root hair elongation, includes key regulators of root hair tip growth, such as MRH6, XTH26, and XTH14, as well as several peroxidases. In particular, changes in redox homeostasis through the altered abundance of peroxidases appear to be important for the root hair phenotype of Pi-deficient plants. This supposition is supported by the observation that the distribution of two major ROS species, H_2O_2 and superoxide, is perturbed in *otu5* mutants (Fig. 8). Further evidence for a role of ROS in the *otu5* phenotype derives from the decreased abundance of the mediator subunit protein PFT1/MED25 in Pi-deficient *otu5* plants. Mutants defective in the expression of *PFT1* form short root hairs due to an imbalance in the distribution of ROS caused by the compromised expression of class III peroxidases (Sundaravelpandian et al., 2013). The short-root-hair phenotype of *pft1* mutants was suppressed by the application of peroxidase and NADPH oxidase inhibitors, suggesting that PFT1 controls root hair growth by maintaining ROS distribution patterns (Sundaravelpandian et al., 2013). Similar to Pi-deficient *otu5* plants, superoxide levels are increased in *pft1* mutants, while H_2O_2 appears to be less abundant. Notably, in *pft1* mutants, *XTH26* was significantly downregulated (Sundaravelpandian et al., 2013). In addition, H_2O_2 treatment induced the expression of *XTH26*, suggesting that XTH26 is a likely target of redox signaling. PIP2;4, another root hair-related protein with altered abundance in *otu5* plants, has been shown to transport H_2O_2 (Dynowski et al., 2008) and, thus, may be critically involved in maintaining ROS balance during root hair morphogenesis. Homozygous *pip2;4* mutants were found to form longer root hairs both under Pi-replete and Pi-deficient conditions (Lin et al., 2011). Thus, decreased PIP2;4 abundance may have contributed to the long-root-hair phenotype of *otu5* plants via altered H_2O_2 levels. Together, these results suggest that alterations in the level and distribution of H_2O_2 dictate the long-root-hair phenotype of *otu5*.

CONCLUSION

In combination with information on PPIs and knowledge derived from previously conducted reverse genetic studies, the results from this study support the view that a specific subset of proteins is required for root hair morphogenesis under Pi-deficient conditions, the activity of which may be controlled at the chromatin level. Our study identified OTU5 as a critical component of this regulation, acting similar to but separate from ARP6 on chromatin organization. A plausible scenario would comprise an effect of OTU5 on the abundance of H2A.Z, acting in concert with ARP6. However, other effects of OTU5 on chromatin organization that contribute to the phenotype of the *otu5* mutant cannot be excluded. The phenotype of *otu5* does not appear to result from a constitutive Pi starvation response, suggesting that OTU5 acts downstream of or independent of Pi signaling. It can be inferred further from the data that ROS homeostasis plays a central role in the induction of the root hair phenotype typical of Pi-deficient plants. Importantly, OTU5-mediated control appears to impact different levels of gene regulation. For example, for most if not all of the chromatin-related proteins, no support for Pi-dependent transcriptional regulation could be inferred from transcriptomic surveys (Lan et al., 2012), whereas the transcription of several root hair-related proteins was shown to be responsive to the Pi supply. Thus, a multifaceted approach comprising disparate omics is mandatory for a comprehensive, systems-level understanding of the responses of plants to environmental signals. OTU5 appears to be involved in the transduction of external signals, causing alterations in root development if dysfunctional. Opposite effects of OTU5 on some root traits in response to the availability of Pi indicate a context-dependent impact of OTU5 on the phenotypic readout that appears to be interlinked with other chromatin-level regulatory processes induced by low Pi availability.

MATERIALS AND METHODS

Plant Growth Conditions

Arabidopsis (*Arabidopsis thaliana*) plants were grown in a growth chamber on solid medium as described by Estelle and Somerville (1987). Seeds of the accession Col-0 and the *otu5* T-DNA insertion mutant (Salk_032407) were obtained from the Arabidopsis Biological Resource Center (Ohio State University). The *arp6-*

1 (SAIL_599_G03) mutant was described previously and was a kind gift from Y.-Y. Charng (Agricultural Biotechnology Research Center, Academia Sinica). Seeds were surface sterilized by immersing them in 5% (v/v) NaOCl for 5 min and 70% (v/v) ethanol for 7 min, followed by four rinses in sterile water. Seeds were placed on petri dishes and kept for 2 d at 4°C in the dark, before the plates were transferred to a growth chamber and grown at 21°C under continuous illumination (50 μmol m^{-2} s^{-1}; Phillips TL lamps). The medium was composed of (mM) KNO_3 (5), $MgSO_4$ (2), $Ca(NO_3)_2$ (2), KH_2PO_4 (2.5) and (μM) H_3BO_3 (70), $ZnSO_4$ (1), $CuSO_4$ (0.5), Na_2MoO_4 (0.2), $CoCl_2$ (0.01), FeEDTA (40), 1% (w/v) MES, supplemented with Suc (43.8 mM), and solidified with 0.4% (w/v) Gelrite pure (Kelco). The pH was adjusted to 5.5. Low-Pi conditions were obtained by growing plants on medium containing 2.5 μM KH_2PO_4, while the Pi concentration of control medium was 2.5 mM KH_2PO_4. The lower concentration of potassium due to the reduced KH_2PO_4 concentration was compensated for by the addition of KCl. Plants were grown on Pi-sufficient (2.5 mM) medium for 7 d and transferred to Pi-sufficient or low-Pi (2.5 μM) medium for another 7 d.

Construction of Transgenic Lines

To overexpress *OTU5* in Col-0 plants, a C-terminal triple HA-tagged *OTU5a* overexpression construct was made in pBI121 (Jefferson et al., 1987). The wild-type *OTU5a* coding sequence was PCR amplified from pET28a-OTU5a (Radjacommare et al., 2014) and subcloned into pBluescript KS+ to give pKS-OTU5a with engineered restriction sites *Sma*I and *Nco*I. To attach a triple HA tag sequence, the *Sma*I-*Nco*I-restricted *OTU5a* coding sequence from pKS-OTU5a was mobilized into corresponding sites in p1239 to give p1239-OTU5a-HA3. The triple HA-tagged *OTU5a* coding sequence was PCR amplified from the p1239-derived plasmids and cloned into pBluescript KS+ to give pKS-OTU5a-HA3 with engineered restriction sites *Sma*I and *Sac*I. The *Sma*I- and *Sac*I-restricted coding sequence of the triple HA-tagged *OTU5a* replaced the GUS coding sequence in pBI121 to give the overexpression construct pBI121-OTU5a-HA3. To complement the *otu5* mutant, the cauliflower mosaic virus 35S promoter in pEN-L4-2-L3 (Ghent University) and the OTU5a coding sequence in pENTR221 (Invitrogen) were mobilized into pKNGSTAP (Ghent University) using three-fragment gateway recombination (Van Leene et al., 2008) to generate the complementation construct. A freeze-thaw method was used to transform *Agrobacterium tumefaciens* GV3101, and the Arabidopsis transformation was performed as described previously (Clough and Bent, 1998). Homozygous complementation and overexpression lines were selected from T3 plants.

qRT-PCR

Root samples were collected from 14-d-old seedlings and frozen immediately in liquid nitrogen. Total RNA was isolated using the RNeasy Mini Kit (Qiagen) and treated with DNase using the TURBO DNA-free Kit (Ambion) as indicated by the manufacturer. cDNA was synthesized using DNA-free RNA with oligo$(dT)_{20}$ primers and the SuperScript III First-Strand Synthesis System for RT-PCR (Invitrogen). After incubation at 50°C for 1 h and subsequently at 70°C for 15 min, 1 μL of RNase H was added and incubated for 20 min at 37°C. The cDNA was used as a PCR template in a 20-μL reaction system using the SYBR Green PCR Master Mix (Applied Biosystems) with programs recommended by the manufacturer in the AB QuantStudio Real Time PCR System (Applied Biosystems). Three independent replicates were performed for each sample. The $\Delta\Delta C_T$ method was used to determine the relative amount of gene expression, with the expression of Elongation Factor1 (EF1) used as an internal control. The following primers were used: for *NPC4* (At3g03530), 5′-GGATTGAGCCTGGCACAGTT-3′ (forward) and 5′-GACGAATGCTCATATTGTGACCTT-3′ (reverse); for *SQD2* (At5g01220), 5′-TCATCTCTGAAATTGCACGGTTT-3′ (forward) and 5′-GCCAGAGCACCAAAGACCAT-3′ (reverse); for *SPX1* (At5g20150), 5′-GAAGAGCACAATCGCTGCCTT-3′ (forward) and 5′-TGGCTTCTTGCTCCAACAATG-3′ (reverse); for *SPX3* (At2g45130), 5′-GCGCCGGTGGAATCTATTTT-3′ (forward) and 5′-GCAACTCCTTGTGGTGGATGA-3′ (reverse); and for *EF1α* (At5g60390), 5′-AACTTTGATGGCGTTTGAGC-3′ (forward) and 5′-TCCGGAAACTGCATAATTGA-3′ (reverse).

Protein Extraction

Roots from 14-d-old Pi-sufficient and Pi-deficient plants were ground in liquid nitrogen and suspended in a 10× volume of precooled acetone (−20°C) containing 10% (v/v) TCA and 0.07% (v/v) 2-mercaptoethanol. Proteins were then precipitated for 2 h at −20°C after thorough mixing. Precipitated proteins were collected by centrifuging at 35,000*g* (JA-20 108 rotor; Beckman J2-HS) at 4°C for 30 min. The supernatant was carefully removed, and the protein pellets were washed twice with cold acetone containing 0.07% (v/v) 2-mercaptoethanol and 1 mM phenylmethanesulfonyl fluoride and a third time with cold acetone. Protein pellets were dried and stored at −80°C or immediately dissolved using protein extraction buffer composed of 8 M urea and 50 mM triethylammonium bicarbonate, pH 8.5, for 1 h at 6°C under constant shaking. Protein extracts were centrifuged at 19,000*g* for 20 min at 10°C. The supernatant was then collected, and the protein concentration was determined using a protein assay kit (Pierce).

In-Solution Trypsin Digestion and iTRAQ Labeling

Total protein (100 μg) was reduced by adding DTT to a final concentration of 10 mM and incubated for 1 h at 37°C. Subsequently, iodoacetamide was added to a final concentration of 50 mM, and the mixture was incubated for 30 min at room temperature in the dark. Then, DTT (final 30 mM) was added to the mixture to consume any free iodoacetamide by incubating the mixture for 1 h at room temperature in the dark. Proteins were then diluted by 50 mM Tris, pH 8, to reduce the urea concentration to 4 M and digested with 250 units mL^{-1} Benzonasae (Sigma) for 2 h at room temperature and digested with 0.5 μg of Lys-C (Wako) for 4 h at room temperature. The Lys-C-digested protein solution was further digested with 20 μg of modified trypsin (Promega) at 37°C overnight after the solution was further diluted with 50 mM Tris, pH 8, to reduce the urea concentration to less than 1 M. The resulting peptide solution was acidified with 10% (v/v) trifluoroacetic acid and desalted on a C18 solid-phase extraction cartridge (Oasis HLB; Waters). Desalted peptides were then labeled with iTRAQ reagents (Applied Biosystems) according to the manufacturer's instructions. Proteins extracted from wild-type roots growing under normal and low-Pi conditions were labeled with reagents 114 and 115, respectively; proteins extracted from *otu5* roots growing under normal and low-Pi conditions were labeled with reagents 116 and 117 individually. Three independent biological experiments were performed. The reaction was allowed to proceed for 1 h at room temperature. Subsequently, treated and control peptides were combined and further fractionated offline using high-resolution strong cation-exchange chromatography (PolySulfoethyl A, 4.6 × 100 mm, 5 μm, 200-Å beads). In total, 50 fractions were collected and combined into 20 final fractions. Each final fraction was lyophilized in a centrifugal speed vacuum concentrator. Samples were stored at −80°C.

Tandem Mass Spectrometry Analysis

Nano-HPLC-MS/MS analysis was performed on a nanoAcquity system (Waters) connected to an LTQ-Orbitrap Elite hybrid mass spectrometer (Thermo Scientific) equipped with a PicoView nanospray interface (New Objective). Peptide mixtures were loaded onto a 75-μm i.d., 25-cm length C18 BEH column (Waters) packed with 1.7-μm particles with a pore size of 130 Å and were separated using a segmented gradient in 150 min from 5% to 40% (v/v) solvent B (acetonitrile with 0.1% (v/v) formic acid) at a flow rate of 300 nL min^{-1} and a column temperature of 35°C. Solvent A was 0.1% (v/v) formic acid in water.

The LTQ-Orbitrap Elite hybrid mass spectrometer was operated in positive ionization mode. The mass spectrometry survey scan for all experiments was performed in the Fourier transform cell with a mass-to-charge ratio (m/z) range between 350 and 1,600. The resolution was set to 120,000 at m/z 400, and the automatic gain control was set to 500,000 ions. The m/z values triggering MS/MS were put on an exclusion list for 90 s. The minimum mass spectrometry signal for triggering MS/MS was set to 5,000. In all cases, one microscan was recorded. For high-energy collision dissociation, the applied acquisition method consisted of a survey scan to detect the peptide ions followed by a maximum of 15 MS/MS experiments of the 15 most intense signals exceeding a minimum signal of 5,000 in survey scans. For MS/MS, we used a resolution of 15,000, an isolation window of 2 m/z, and a target value of 50,000 ions, with maximum accumulation times of 250 ms. Fragmentation was performed with normalized collision energy of 35% and an activation time of 0.1 s. For each experiment, two technical repeats were performed.

Database Search and Quantification

Two search algorithms, Mascot (version 2.4; Matrix Science) and SEQUEST, which is integrated in Proteome Discoverer software (version 1.4; Thermo Scientific), were used to simultaneously identify and quantify proteins. Searches were made against the Arabidopsis protein database (TAIR10 20110103, 27,416

sequences; ftp://ftp.arabidopsis.org/home/tair/Sequences/blast_datasets/TAIR10_blastsets/TAIR10pep 20110103 representative gene model) and a decoy database containing the reversed sequences of the original database for peptide spectrum match FDR calculation. For biological repeats, spectra from the two technical repeats were combined into one file and searched. The search parameters were as follows: trypsin was chosen as the enzyme with two missed cleavages allowed; fixed modifications of carbamidomethylation at Cys and iTRAQ4plex at Lys and peptide N terminus; variable modifications of oxidation at Met and iTRAQ4plex at Tyr; peptide tolerance was set at 10 ppm, and MS/MS tolerance was set at 0.05 D. The search results were passed through additional filters before exporting the data. For protein identification, the filters were set as follows: peptide target FDR at least 0.05 (with 95% confidence) and delta Cn better than 0.15. For protein quantitation, only unique peptides were used to quantify proteins. Resulting protein ratios were normalized on protein median.

Statistical Analysis

Proteins with significant changes in abundance upon different genotypes and Pi deficiencies were selected using a method described by Cox and Mann (2008). In brief, the mean and SD from the $\log_2$ ratios of the more than 10,000 quantified proteins overlapping in two biological repeats was calculated. Next, 95% confidence (Z score = 1.96) was used to select those proteins whose distribution was removed from the main distribution. For the down-regulated proteins, the confidence interval was calculated by the following formula: confidence interval = mean ratio of the identified proteins − 1.96×SD, corresponding to a protein ratio of 0.616837. Similarly, for the up-regulated proteins, the mean confidence interval was calculated by the following formula: mean ratio + 1.96×SD. Protein ratios outside this range were defined as being significantly different at $P = 0.05$ and used as the cutoff value for the down-regulated proteins and the up-regulated proteins.

Root Hair Density and Length Measurement

Root hair density was determined in a zone between 2 and 6 mm above the root tip. Root hair length was measured starting from 2 mm above the root tip. At least 100 root hairs were measured for each root from five or more plants per growth type or genotype.

ChIP Analysis

Roots of 14-d-old-day seedlings were used for ChIP analysis. H2A.Z antibody (ab4174; Abcam) was used at a dilution of 1:100. DNA was analyzed by real-time PCR with the *ACT2* 3′ untranslated region sequence as the endogenous control for all ChIP experiments. The Ct value was recorded in the experimental report after analysis by QuantStudio 12K Flex software. Ct values were used to calculate the fold changes between samples and normalized input ΔCt (normalized to the input samples) value for each sample. ΔCt [normalized ChIP] = (Ct [ChIP] − (Ct [Input] − Log2 (input dilution factor))), using the following equation: ΔCt [normalized ChIP] = (Ct [ChIP] − (Ct [Input] − Log2 (input dilution factor))). Finally, the percentage (Input %) value for each sample is calculated as follows: Input % = 2 (−ΔCt [normalized ChIP]) × 100. Relative enrichment was calculated by setting the H2A.Z enrichment of Pi-replete wild-type roots as 100%. The following primers were used: for *XTH26* (At4g28850), 5′-GATCTGCTATTAAATCAAAGGTGG-3′ (forward); for *XTH26* (At4g28850), 5′-TAATAGGCTGCAACGGTTCC-3′ (reverse); for *FRG4* (At1g61140), 5′-CCTGCTCATACTTGCTCTGC-3′ (forward); and for *FRG4* (At1g61140), 5′-GGCCATCATATTGCCATCAGG-3′ (reverse).

Determination of ROS Levels and Distribution

For superoxide staining, 10 to 20 roots of 14-d-old seedlings were incubated under vacuum in 10 mM sodium azide for 10 min. Then, the seedlings were stained for 25 min in a solution containing 2 mM NBT in 20 mM phosphate buffer (pH 6.1). Subsequently, seedlings were placed in destaining solution for 40 min. Roots were mounted on a glass slide with a drop of double distilled water and a coverslip and then observed with a Zeiss Axio Imager Z1 fluorescence microscope equipped with an AXIOCAM 506 MONO CCD camera that was used to capture photographs.

H_2O_2 was visualized by incubating 10 to 20 roots of 14-d-old seedlings for 2 min in a solution containing 5 μM HPF (Sigma) in 0.1 M phosphate buffer (pH 6.1). Roots were mounted on a glass slide with a drop of double distilled water and a coverslip and then observed with a laser scanning microscope (Zeiss LSM 510 META). An argon ion laser was used for excitation at 488 nm; the emission fluorescence was captured using the 500- to 550-nm bandpass for HPF fluorescence. Photographs were captured with 10× magnification. HPF fluorescence between different samples was imaged using the same laser intensity and scanning settings. Integrated density (= area × mean gray value) was used to measure H_2O_2 intensity.

Supplemental Data

The following supplemental materials are available.

Supplemental Figure S1. Analysis of Pi status.

Supplemental Figure S2. H2A.Z occupancy in the CDS of *FRG4* and *XTH26*.

Supplemental Data Set S1. Differentially expressed proteins.

ACKNOWLEDGMENTS

We thank Dr. Thomas J. Buckhout (Humboldt Universität Berlin) for critical comments on the article. Proteomic mass spectrometry analyses and in-gel digestion were performed by the Proteomics Core Laboratory sponsored by the Institute of Plant and Microbial Biology and the Agricultural Biotechnology Research Center, Academia Sinica.

Received October 26, 2017; accepted January 2, 2018; published January 4, 2018.

LITERATURE CITED

Berr A, Shafiq S, Pinon V, Dong A, Shen WH (2015) The trxG family histone methyltransferase SET DOMAIN GROUP 26 promotes flowering via a distinctive genetic pathway. Plant J **81:** 316–328

Chandrika NN, Sundaravelpandian K, Yu SM, Schmidt W (2013) ALFIN-LIKE 6 is involved in root hair elongation during phosphate deficiency in Arabidopsis. New Phytol **198:** 709–720

Chen CY, Schmidt W (2015) The paralogous R3 MYB proteins CAPRICE, TRIPTYCHON and ENHANCER OF TRY AND CPC1 play pleiotropic and partly non-redundant roles in the phosphate starvation response of *Arabidopsis* roots. J Exp Bot **66:** 4821–4834

Chiou TJ, Lin SI (2011) Signaling network in sensing phosphate availability in plants. Annu Rev Plant Biol **62:** 185–206

Choi K, Park C, Lee J, Oh M, Noh B, Lee I (2007) *Arabidopsis* homologs of components of the SWR1 complex regulate flowering and plant development. Development **134:** 1931–1941

Clough SJ, Bent AF (1998) Floral dip: a simplified method for *Agrobacterium*-mediated transformation of *Arabidopsis thaliana*. Plant J **16:** 735–743

Coleman-Derr D, Zilberman D (2012) Deposition of histone variant H2A.Z within gene bodies regulates responsive genes. PLoS Genet **8:** e1002988

Cox J, Mann M (2008) MaxQuant enables high peptide identification rates, individualized p.p.b.-range mass accuracies and proteome-wide protein quantification. Nat Biotechnol **26:** 1367–1372

Datta S, Prescott H, Dolan L (2015) Intensity of a pulse of RSL4 transcription factor synthesis determines *Arabidopsis* root hair cell size. Nat Plants **1:** 15138

Dunand C, Crèvecoeur M, Penel C (2007) Distribution of superoxide and hydrogen peroxide in *Arabidopsis* root and their influence on root development: possible interaction with peroxidases. New Phytol **174:** 332–341

Dynowski M, Schaaf G, Loque D, Moran O, Ludewig U (2008) Plant plasma membrane water channels conduct the signalling molecule H_2O_2. Biochem J **414:** 53–61

Estelle MA, Somerville C (1987) Auxin-resistant mutants of *Arabidopsis thaliana* with an altered morphology. Mol Gen Genet **206:** 200–206

Hayashi S, Ishii T, Matsunaga T, Tominaga R, Kuromori T, Wada T, Shinozaki K, Hirayama T (2008) The glycerophosphoryl diester phosphodiesterase-like proteins SHV3 and its homologs play important roles in cell wall organization. Plant Cell Physiol **49:** 1522–1535

Isono E, Nagel MK (2014) Deubiquitylating enzymes and their emerging role in plant biology. Front Plant Sci **5:** 56

Jefferson RA, Kavanagh TA, Bevan MW (1987) GUS fusions: β-glucuronidase as a sensitive and versatile gene fusion marker in higher plants. EMBO J **6:** 3901–3907

Kandasamy MK, Deal RB, McKinney EC, Meagher RB (2005) Silencing the nuclear actin-related protein AtARP4 in *Arabidopsis* has multiple effects on plant development, including early flowering and delayed floral senescence. Plant J **41:** 845–858

Krichevsky A, Zaltsman A, Lacroix B, Citovsky V (2011) Involvement of KDM1C histone demethylase-OTLD1 otubain-like histone deubiquitinase complexes in plant gene repression. Proc Natl Acad Sci USA **108:** 11157–11162

Kuo HF, Chang TY, Chiang SF, Wang WD, Charng YY, Chiou TJ (2014) Arabidopsis inositol pentakisphosphate 2-kinase, AtIPK1, is required for growth and modulates phosphate homeostasis at the transcriptional level. Plant J **80:** 503–515

Lan P, Li W, Lin WD, Santi S, Schmidt W (2013) Mapping gene activity of *Arabidopsis* root hairs. Genome Biol **14:** R67

Lan P, Li W, Schmidt W (2012) Complementary proteome and transcriptome profiling in phosphate-deficient *Arabidopsis* roots reveals multiple levels of gene regulation. Mol Cell Proteomics **11:** 1156–1166

Lázaro A, Gómez-Zambrano A, López-González L, Piñeiro M, Jarillo JA (2008) Mutations in the *Arabidopsis* SWC6 gene, encoding a component of the SWR1 chromatin remodelling complex, accelerate flowering time and alter leaf and flower development. J Exp Bot **59:** 653–666

Lee WY, Lee D, Chung WI, Kwon CS (2009) Arabidopsis ING and Alfin1-like protein families localize to the nucleus and bind to H3K4me3/2 via plant homeodomain fingers. Plant J **58:** 511–524

Li WF, Perry PJ, Prafulla NN, Schmidt W (2010) Ubiquitin-specific protease 14 (UBP14) is involved in root responses to phosphate deficiency in *Arabidopsis*. Mol Plant **3:** 212–223

Lin WD, Liao YY, Yang TJW, Pan CY, Buckhout TJ, Schmidt W (2011) Coexpression-based clustering of Arabidopsis root genes predicts functional modules in early phosphate deficiency signaling. Plant Physiol **155:** 1383–1402

Ma Z, Bielenberg DG, Brown KM, Lynch JP (2001) Regulation of root hair density by phosphorus availability in *Arabidopsis thaliana*. Plant Cell Environ **24:** 459–467

March-Díaz R, García-Domínguez M, Lozano-Juste J, León J, Florencio FJ, Reyes JC (2008) Histone H2A.Z and homologues of components of the SWR1 complex are required to control immunity in *Arabidopsis*. Plant J **53:** 475–487

Müller M, Schmidt W (2004) Environmentally induced plasticity of root hair development in Arabidopsis. Plant Physiol **134:** 409–419

Parker JS, Cavell AC, Dolan L, Roberts K, Grierson CS (2000) Genetic interactions during root hair morphogenesis in *Arabidopsis*. Plant Cell **12:** 1961–1974

Pei W, Du F, Zhang Y, He T, Ren H (2012) Control of the actin cytoskeleton in root hair development. Plant Sci **187:** 10–18

Peña MJ, Kong Y, York WS, O'Neill MA (2012) A galacturonic acid-containing xyloglucan is involved in *Arabidopsis* root hair tip growth. Plant Cell **24:** 4511–4524

Pouteau S, Ferret V, Gaudin V, Lefebvre D, Sabar M, Zhao G, Prunus F (2004) Extensive phenotypic variation in early flowering mutants of Arabidopsis. Plant Physiol **135:** 201–211

Radjacommare R, Usharani R, Kuo CH, Fu H (2014) Distinct phylogenetic relationships and biochemical properties of *Arabidopsis* ovarian tumor-related deubiquitinases support their functional differentiation. Front Plant Sci **5:** 84

Salazar-Henao JE, Lin WD, Schmidt W (2016) Discriminative gene co-expression network analysis uncovers novel modules involved in the formation of phosphate deficiency-induced root hairs in *Arabidopsis*. Sci Rep **6:** 26820

Savage N, Yang TJ, Chen CY, Lin KL, Monk NA, Schmidt W (2013) Positional signaling and expression of ENHANCER OF TRY AND CPC1 are tuned to increase root hair density in response to phosphate deficiency in *Arabidopsis thaliana*. PLoS ONE **8:** e75452

Setsukinai K, Urano Y, Kakinuma K, Majima HJ, Nagano T (2003) Development of novel fluorescence probes that can reliably detect reactive oxygen species and distinguish specific species. J Biol Chem **278:** 3170–3175

Smith AP, Jain A, Deal RB, Nagarajan VK, Poling MD, Raghothama KG, Meagher RB (2010) Histone H2A.Z regulates the expression of several classes of phosphate starvation response genes but not as a transcriptional activator. Plant Physiol **152:** 217–225

Sridhar VV, Kapoor A, Zhang K, Zhu J, Zhou T, Hasegawa PM, Bressan RA, Zhu JK (2007) Control of DNA methylation and heterochromatic silencing by histone H2B deubiquitination. Nature **447:** 735–738

Stetter MG, Schmid K, Ludewig U (2015) Uncovering genes and ploidy involved in the high diversity in root hair density, length and response to local scarce phosphate in *Arabidopsis thaliana*. PLoS ONE **10:** e0120604

Sundaravelpandian K, Chandrika NN, Schmidt W (2013) PFT1, a transcriptional Mediator complex subunit, controls root hair differentiation through reactive oxygen species (ROS) distribution in Arabidopsis. New Phytol **197:** 151–161

Van Leene J, Witters E, Inzé D, De Jaeger G (2008) Boosting tandem affinity purification of plant protein complexes. Trends Plant Sci **13:** 517–520

Wang H, Liu C, Cheng J, Liu J, Zhang L, He C, Shen WH, Jin H, Xu L, Zhang Y (2016) *Arabidopsis* flower and embryo developmental genes are repressed in seedlings by different combinations of polycomb group proteins in association with distinct sets of *cis*-regulatory elements. PLoS Genet **12:** e1005771

Xu Y, Gan ES, Zhou J, Wee WY, Zhang X, Ito T (2014) *Arabidopsis* MRG domain proteins bridge two histone modifications to elevate expression of flowering genes. Nucleic Acids Res **42:** 10960–10974

Yang P, Smalle J, Lee S, Yan N, Emborg TJ, Vierstra RD (2007) Ubiquitin C-terminal hydrolases 1 and 2 affect shoot architecture in *Arabidopsis*. Plant J **51:** 441–457

Yi H, Sardesai N, Fujinuma T, Chan CW, Veena, Gelvin SB (2006) Constitutive expression exposes functional redundancy between the *Arabidopsis* histone H2A gene HTA1 and other H2A gene family members. Plant Cell **18:** 1575–1589